# Focusing characteristics of high voltage electron gun under variable electromagnetic and beam source parameters

**LI SHENGBO**
Xiamen University of Technology
**QIU YUFAN**
Xiamen University of Technology
**FU SHENGPING** ( 7025370@163.com )
Jimei University
**SHUTIN DENIS**
Orel State University n.a. I.S. Turgenev
**SONG YE**
Xiamen University of Technology
**CHANG JIAWEI**
Xiamen University of Technology
**BAI FENGMIN**
Heibei Zhicheng High Energy Beam Technology Co., Ltd

**Article**

**Keywords:** electron gun, beam source parameters, focus characteristics, waist diameter, beam spot diameter

**Posted Date:** May 17th, 2022

**DOI:** https://doi.org/10.21203/rs.3.rs-1625088/v1

# Focusing characteristics of high voltage electron gun under variable electromagnetic and beam source parameters

**LI SHENGBO[1], QIU YUFAN[1], FU SHENGPING[2,*], SHUTIN DENIS [3], SONG YE[1], CHANG JIAWEI[1], BAI FENGMIN,[4]**

[1]*School of Mechanical and Automotive Engineering, Xiamen University of Technology, 361024, Xiamen, Fujian, China*
[2]*College of Marine Equipment and Mechanical Engineering, Jimei University, 361021, Xiamen, Fujian, China*
[3]*Orel State University n.a. I.S. Turgenev, Department of Mechatronics, Mechanics and Robotics, 302026, Orel, Russia*
[4]*Heibei Zhicheng High Energy Beam Technology Co., Ltd.,065300, Langfang, Hebei, China*

**Abstract:** The focusing characteristics of electron guns sufficiently affect the quality of electron beam welding. At present, no systematic theoretical method calculates the beam waist and beam spot parameters that reflect the focusing characteristics of electron gun. Aiming at this problem, this paper contains a theoretical analysis of the relationship among the potential on the electron gun axis, the diameter of beam waist, and the trajectory of charged particles that pass through the focusing coil. A simulation model based on a F19-01 high-voltage electron gun for this study is developed using the CST simulation platform. The model simulates the variation of electron beam waist and beam spot diameter under different electrostatic focusing and magnetic focusing parameters. Results of a single-parameter study show that an increase in the cathode-to-anode distance leads to the increment in the beam spot diameter, whereas an increase in the bias cup aperture, as well as increases in anode aperture and focusing current, cause its decrease. An orthogonal test confirms that the aspect ratio of the electron beam welding seam under the same power can be improved effectively by selecting the cathode-to-anode distance of 28.4 mm, the bias cup aperture of 6 mm, and the anode aperture of 10 mm. Thus, the experimental data prove the correctness of the theoretical and simulation analyses.

**Key words:** electron gun; beam source parameters; focus characteristics; waist diameter; beam spot diameter

## 1. Introduction

Beam spot is the focal point of the electron beam focused on the welding work surface. The beam spot is an important indicator that reflects the focusing characteristics of the electron gun. When the beam size is the same, smaller beam spot diameter means more concentrated energy. And the weld seam width reduces the heat reaction zone of the weld to improve the quality of welding. Therefore, studying the influence of beam source and electromagnetic structure parameters on the beam spot size is crucial to develop higher performance electron guns[1-2].

At present, the research on electron gun beam spot mainly focuses on how to simulate the effects of electron gun voltage, bias cup internal arc, and other parameter on the electron beam spot. Both finite element analysis method and relevant theoretical models are adopted. Wang et al. calculated the effect of different model structures on beam spot and beam flow by analyzing electric field theory[3-4]. Wang et al. used simulation software to simulate the variation of electron beam spot and beam current under different structural parameters[5-8]. Xin verified the desired electron gun performance by using different electronic simulation software designs [9-11]. Kornilov et al. determined the optimal operating parameters by studying

the electron gun emission pattern [12-14]. Xu et al. first obtained the required parameters of the focusing coil by theoretical calculation and the required results by simulation [15]. Feng analyzed the influence of the leakage field of the focusing coil on the beam current and reduced the influence of the leakage field through corresponding measures to ensure beam quality [16]. Yin et al. conducted a detailed theoretical study on the magnetic field part of the electron gun. And the results were verified and optimized by using a 3D particle simulation program[17].

In summary, the current research on electron gun beam spot under different electron gun voltages and bias cup internal arcs is mainly focused on theoretical analysis and simulation research. The effect of beam source structure and electromagnetic parameters on beam spot is seldom studied. Therefore, the beam source structure of domestic F19-01 high-voltage electron gun is taken as an example. Both the theory and CST simulation model of electron gun are established. The influences of the change of the beam source structure on the electron gun axis potential and the trajectory of the electron beam when it passes through the focusing coil under the same beam current are theoretically analyzed. Eventually the theoretical analysis results are verified by single-parameter tests. Moreover, orthogonal tests are designed to explore the influences of different structures on the beam spot size quantitatively.

## 2. Electron gun focus principle

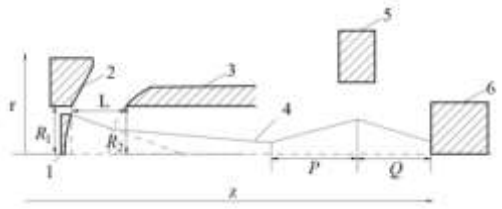


1-cathode 2-bias cup 3-anode 4-beam path 5-focusing coil 6-workpiece R1-bias cup hole radius L-distance between anode and cathode R2-anode hole radius P-distance from waist to magnetic center Q-distance from beam spot to center surface of magnetic lens

Fig.1 Brief diagram of electron beam focusing path

As shown in Fig.1, cathode 1 is heated so that charged particles overflow its surface. When the charged particles pass through the high-voltage electric field generated by the beam source structure, they are continuously converged by the electric field force. As the charged particles approach each other, the space charge force also increases. After the beam enters anode 3, the velocity of the charged particles that pass through the high-voltage electric field, which is directed to the axis, decreases continuously under the force of space charges, and a beam waist where the velocity is zero is generated. After that, the electron beam passes through the internal channel of the anode in an emission shape. A current is inputted to the focusing coil. A focusing magnetic field occurs in the center of the coil, and the divergent electron beam current is focused on the surface of the welding workpiece to obtain a beam spot.

According to the effect of the electromagnetic lens on the electron beam current, the beam spot radius of the electron beam and the beam waist radius satisfy the following formula.

$$r_1 = \frac{Q}{P} r_2 , \tag{1}$$

where $r_1$ is the beam spot radius of the electron beam, $r_2$ is the band beam waist radius, $P$ is the distance from the beam waist to the central plane of the magnetic lens, and $Q$ is the distance from the beam spot to the central plane of the magnetic lens.

The fixed welding height does not change in the actual welding process. And $Q$ is regarded as a constant. According to experience, the distance between the beam waist and the center of the magnetic lens is approximately 500 mm. And the changes in the beam source structure parameters make the position of the beam waist vary within a few millimeters. Thus, $Q/P$ is approximately regarded as a constant value. The waist is approximately linear. When the size of the electron beam spot is difficult to measure, the influences of different beam source structures on the beam waist radius are analyzed theoretically, which reflect the variation characteristics of the beam spot under different beam source structure parameters.

Only the effect of the electric field in the paraxial region on the electrostatic focusing of the electron beam needs to be considered because the electron beam current only moves in the paraxial region. According to the force analysis of charged particles in the electric field, the following formula is obtained.

$$\begin{cases} F_z = -eE_z = eV'_z \\ F_r = -eE_r = -\dfrac{re}{2}V''_z \end{cases}, \tag{2}$$

where $E$ is the electric field strength, e is the amount of electron charge, $V'$ is the electric field, and $V''_z$ is the focusing strength.

According to Formula (2), the force on the charged particle in the r direction depends on the magnitude of $V''_z$. When $V''_z>0$, the greater $V''_z$ is, the greater the convergence degree of the electron beam will be.

According to the space potential equation under the first type of boundary conditions solved by Wang et al. 18, the general expression of the on-axis potential $V_z$ is:

$$\begin{aligned} Vz = {} & \frac{\sigma}{c\pi}[(z+a)\arctan(\frac{z+a}{R_1}) - (z-a)\arctan(\frac{z-a}{R_1})] + \frac{1-\sigma}{c\pi}[(z+\beta)\arctan(\frac{z+\beta}{R_2}) - \\ & (z-\beta)\arctan(\frac{z-\beta}{R_2}) - (z+\alpha)\arctan(\frac{z+\alpha}{R_1}) + (z-\alpha)\arctan(\frac{z-\alpha}{R_1})] \end{aligned}, \tag{3}$$

where $a$ is the increase of the bias cup-anode distance, $b$ is the thickness of the bias cup, $c$ is the increase of the bias cup-cathode distance, $R_1$ is the radius of the bias cup hole, $R_2$ is the radius of the anode hole, σ is the bias cup potential, $\alpha=a+b$, and $\beta=a+b+c$.

In the Formula (3), the parameters, such as $R_1$, $R_2$, $b$, $a$, and $c$, are taken as the actual working conditions, among which the cathode potential, the bias cup potential, and the anode potential are taken as −150000, −151600, and 0 V respectively. After solved in MATLAB, the changes in $V''_z$ under different beam source structure parameters and the same beam current are analyzed theoretically, as shown in Fig.2.

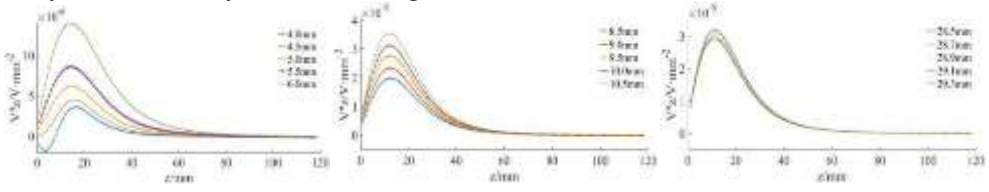

(a) Bias cup aperture (b) Cathode-anode distance (c) Anode aperture

Fig.2 Influence of different beam source structures on focusing strength

It can be seen from Fig.2 that the focus intensity $V''_z$ of the on-axis potential first increases with the increase of the on-axis distance, and gradually decreases to zero after reaching the

maximum focus intensity. Combining equation (2) and Fig.2, it can be seen that with the increase of the bias cup aperture and the anode aperture, $V''_z$ is increasing under the same beam current, that is, the higher the degree of convergence the electron beam is subjected to, the smaller the beam waist radius. With the increase of the anode aperture, $V''_z$ keeps increasing, that is, the higher the convergence degree of the electron beam, the smaller the beam waist radius. Moreover, with the increase of the cathode-anode distance, $V''_z$ decreases continuously. And both the convergence degree of the electron beam and the beam waist radius decrease continuously. According to the formula (1), it can be obtained that the beam spot radius of the electron beam decreases continuously with the increase of the bias cup aperture and the anode aperture. With the increase of the distance between the cathode and the anode, the beam spot radius increases continuously.

After leaving the beam source structure, the charged particles are gradually dispersed due to only the mutual space charge force. And they need to pass through the focusing coil for secondary focusing to make the focus fall on the weld. Since the focusing coil generates an inhomogeneous magnetic field after energizing, its magnetic field is simplified in the theoretical analysis as the magnetic induction intensity $B$, which continuously increases the magnetic field along the $z$ direction, $B=B_0 \cdot z$. Assuming its mass is m, a charged particle with a charge quantity q is shown in Fig.3.

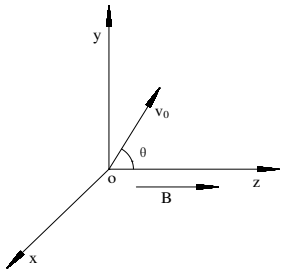


Fig.3 Charged particles enter an inhomogeneous magnetic field

At the speed of $v_0$, it enters the magnetic field from the coordinate origin. The angle between the speed direction and the z axis is $\theta$. On the hypothesis of ignoring gravity, the charged particles are only affected by the Loren magnetic force in the magnetic field. The equation of motion is expressed as follows.

$$m\frac{dv}{dt} = qvB. \tag{4}$$

Velocity $v=v_z i+v_y j+v_x k$ and $B=B_0 \cdot zi$ is substituted into Formula (4) to obtain the three directions vectors:

$$\begin{cases} m\dfrac{dv_x}{dt} = -qB_0 v_y z \\ m\dfrac{dv_y}{dt} = qB_0 v_x z \\ m\dfrac{dvz}{dt} = 0 \end{cases}. \tag{5}$$

According to the relationship between position and velocity, the equation is obtained as follows.

$$\begin{cases} \dfrac{dx}{dt} = v_x \\ \dfrac{dy}{dt} = v_y \\ \dfrac{dz}{dt} = v_z \end{cases} . \tag{6}$$

When $t$=0, The initial conditions are: $x$=$y$=$z$=0, $v_z$=$v_0\cos\theta$, $v_y$=$v_0\sin\theta$, and $v_x$=0, MATLAB software is used to substitute Formulas (5) and (6) into Formula (4). The trajectory of the charged particle in the non-uniform magnetic field can be obtained at this time. When $v_0$=500 m/s, $\theta$=60°, and $qB_0/m$=1000, the particle trajectory is shown in Fig.4.

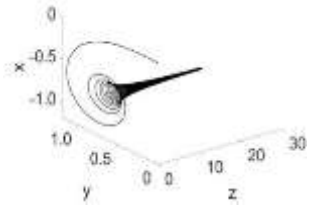


Fig.4 Particle trajectories

Fig.4 shows that the trajectory of the charged particles in the magnetic field that is continuously strengthened along the $Z$ direction is a spiral with a gradually decreasing radius. And a space charge force exists between the charged particles. Thus, the particle beam will diverge again after leaving the focusing coil. And the thinnest position of the beam is defined as the beam spot in this process. The influence of electromagnetic parameters on the beam spot based on aforementioned theoretical formulas is not clear because the actual magnetic field is more complicated than that of theoretical description. Therefore, CST simulation analysis is used to study the variation law of the beam spot under different electromagnetic parameters.

## 3. Simulation verification

### *3.1 Simulation model*

According to the structural parameters of the experimental equipment F19-01 high-voltage electron gun, the three-dimensional models of the cathode, anode, bias cup, and focusing coil of the electron gun are established in Pro/E (shown as Fig.5). The following assumptions are adopted: 1) Because the beam source structure is mainly studied, the materials of the cathode, anode, and bias cup are set to PEC (ideal conductive and magnetic material); and 2)The axis of the electron gun overlapped by default. The cathode is equated to a thin circular sheet with the same emitting surface area because charged particles are emitted only from the cathode surface.

a) Cathode b) Bias cup c) Anode d）Focusing coil

Fig.5 Beam source structure and focusing component

The 3D part model of Pro/E is imported into the CST. And then the simulation model of electron gun is established by assembling according to the actual dimensions. Its spatial dimension is shown in Fig.6. The cathode is located 0.3mm below the opening in the center of the bias cup, and the focusing coil is 451mm from the anode bottom.

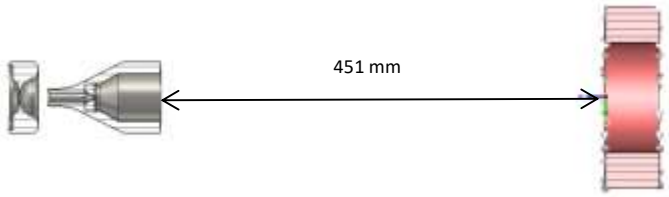


Fig.6 Model structure drawing

### *3.2 Effect of different parameters on beam spot*

The CST Particle Studio module is used to simulate the whole process of electron beam emission from electron gun to verify the accuracy of the theoretical model. Simulation conditions: acceleration voltage is of 120 kV, beam current is of 50mA, and the number of cathode emission particles is 10000.

#### *3.2.1 Bias cup aperture*

According to the actual welding conditions, the cathode distance and the anode aperture are set as 29.3 mm and 10 mm. And the bias cup aperture is taken as 4, 4.5, 5, 5.5, and 6 mm respectively. The cross-section size of the same beam flow at the same location (shown as Fig.7) is obtained when the bias cup aperture changes based on CST software simulation model.

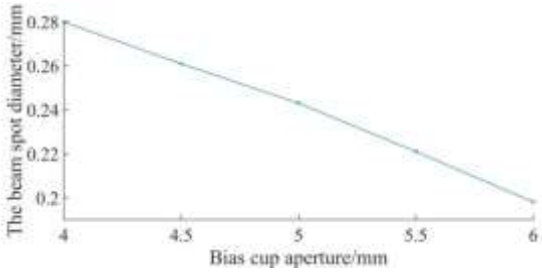


Fig.7 Beam spot diameter with different bias cup aperture

As shown in Fig.7, the electron beam spot diameter decreases from 0.280mm to 0.198mm as the bias cup aperture increases from 4.0mm to 6.0mm with an overall decreasing trend.

#### *3.2.2 Cathode-anode distance*

According to the actual welding conditions, the bias cup aperture and the anode aperture are set to 10mm and 10mm respectively; the cathode-anode distance is set as 28.5, 28.7, 28.9, 29.1, and 29.3mm. The cross-section size of the same beam flow at the same location (shown as Fig.8) is obtained when the distance between cathode and anode changes based on CST software simulation model.

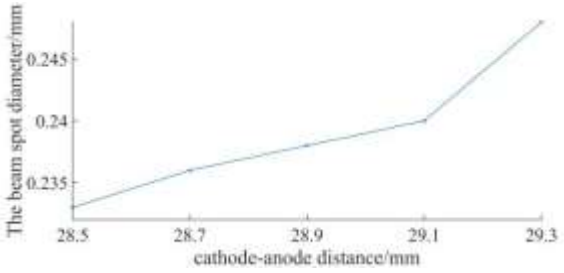


Fig. 8 Beam spot diameter with different distances between anode and cathode

Fig. 8 shows that the electron beam spot diameter increased from 0.233mm to 0.248mm as the cathode-anode distance from 28.5mm to 29.3mm with an overall increasing trend.

### *3.2.3 Anode aperture*

According to actual welding conditions, the bias cup aperture and cathode distance are set as 10mm and 29.3mm respectively; and the anode aperture are taken as 8.5, 9, 9.5, 10, and 10.5mm. The cross-section size of the same beam flow at the same location (shown as Fig.9) is obtained when the anode aperture changes based on CST software simulation model.

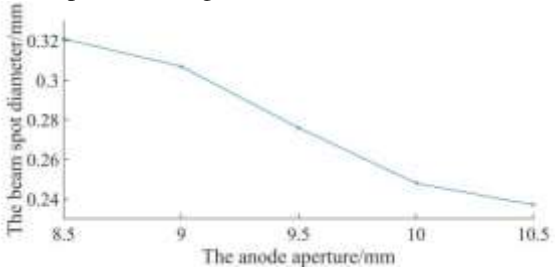


Fig.9 Beam spot diameter with different anode aperture

As shown in Fig.9, the electron beam spot diameter decreases from 0.321mm to 0.237mm as the anode aperture diameter increases from 8.5 mm to 10.5 mm, with an overall decreasing trend.

### *3.2.4 Focusing coil position*

Restricted by the internal structure of the electron gun, the distance between the focusing coil and the cathode emitting surface is at least 400mm. Thus, the beam source parameters are set the same, and the distances between the focusing coil and the cathode emitting surface are taken as 400, 425, 450, 475, and 500mm. The cross-section size of the same beam flow at different focusing coil positions (shown as Fig.10) is obtained based on CST software simulation model.

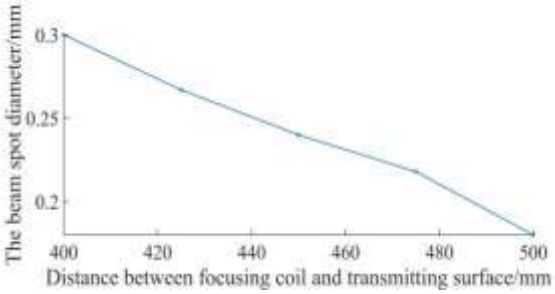

Fig.10 Influence of focusing coil position on beam spot

As seen from Fig.10, the beam spot diameter gradually decreases from 0.30mm to 0.18mm with the increase in distance between the focusing coil and the emitting surface of the cathode within the selected distance.

### *3.2.5 Focusing coil current*

The same beam source parameters are set, and the focusing coil currents are taken as 3.0, 3.1, 3.2, 3.3, and 3.4A in the range of focusing coil currents used. The cross-section size of the same beam flow at different focusing coil currents (shown as Fig.11) is obtained based on CST software simulation model.

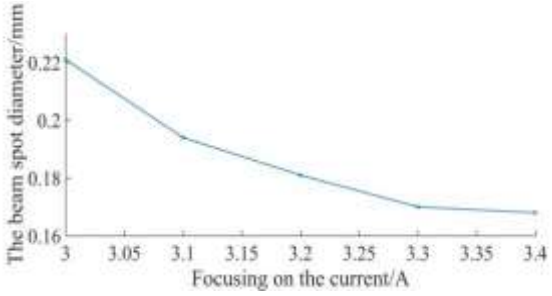


Fig.11 Effect of focusing coil current on beam spot

Fig.11 shows that the beam spot diameter gradually decreases from 0.22mm to 0.17mm as the focusing current increases from 3.0A to 3.4A within the selected focusing current range.

## 4. Experimental verification

To verify the accuracy of the theoretical calculation and simulation model, a single-variable experiment is designed for the F19-01 electron gun to explore the influences of the bias cup aperture, the cathode-anode distance, and the anode aperture on the beam spot size. As shown in Fig.12. The test parameters are set as follows: accelerating voltage U=120 kV, beam current I=50mA, welding speed 800mm/min, welding height 330mm, and test plate material 1Cr18Ni9Ti. Because the beam spot size cannot be measured during welding, the aspect ratio of the weld is adopted as the experimental index. Under the same beam current, the larger the aspect ratio of the weld is, the smaller the beam spot will be.

a) Anode b) Bias cup

Fig.12 Anodes and bias cups with different pore sizes

As the volume of the test plate is too small relative to the vacuum chamber, in order to make the test plate can be located within the effective working distance of the electron gun, it is necessary to fix the metal block on the table and clamp the test plate on the metal block so that it will not move when the table is moved. The clamping method is shown in Fig.13.

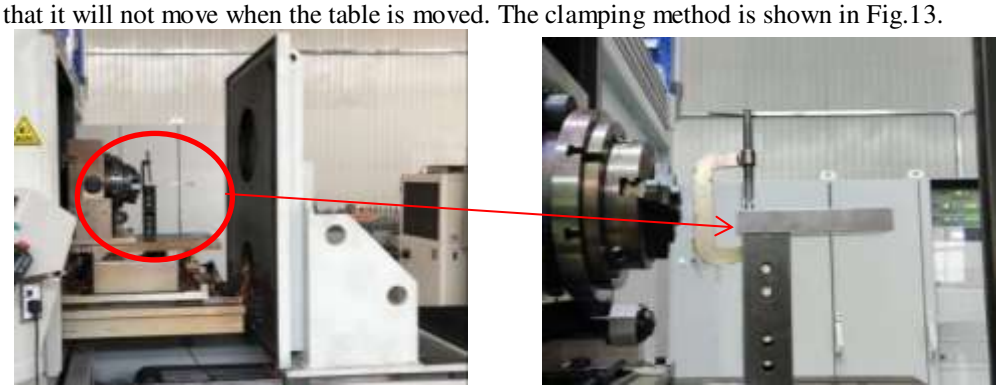

Fig.13 Test plate clamped

### *4.1 Bias cup aperture*

To study the influence of bias cup aperture on the the aspect ratio of the weld, the bias cup aperture is 4, 4.5, 5, 5.5, and 6mm for testing. Moreover, The distance between the cathode and anode is 29.3mm, and the anode diameter is 10 mm. The variation law of the welding seam aspect ratio with the diameter of the bias cup is obtained (shown as Fig.14).

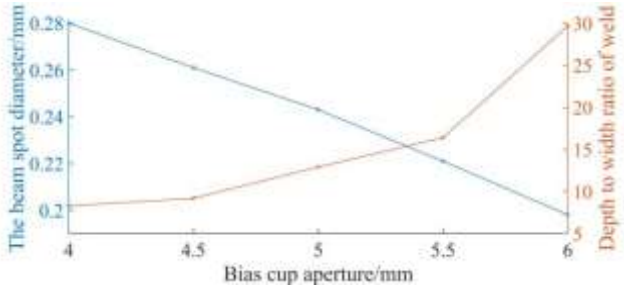


a）Influence of bias cup aperture on depth to width ratio of weld

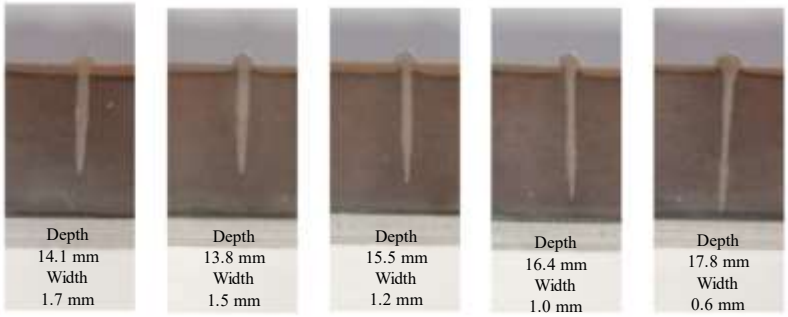


b）Weld quality analysis

Fig.14 Welding line with different bias cup aperture

Fig.14 shows that within the selected range, as the diameter of the bias cup increases from 4.0 mm to 6.0 mm, the aspect ratio of the weld increases from 8.29 to 29.7. Combined with the simulation results: the beam spot diameter decreases from 0.28 to 0.198mm. The conclusion can be drawn: which proves that under the same beam current, with the increase in bias cup aperture, the diameter of the beam spot becomes smaller，eventually leading to an increase in the weld depth to width ratio.

### *4.2 Cathode-anode distance*

To study the influence of the cathode-anode distance on the the aspect ratio of the weld, the influence of the cathode-anode distance is 28.5, 28.7, 28.9, 29.1, and 29.3 mm for testing. Moreover, the diameter of the bias cup is 29.3 mm, and the diameter of the anode is 10 mm. The variation law of the weld aspect ratio with the distance between the cathode and anode is obtained (shown as Fig.15).

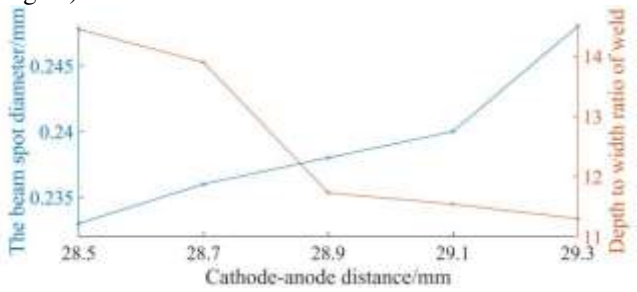


a）Influence of anode and cathode distance on depth to width ratio of weld

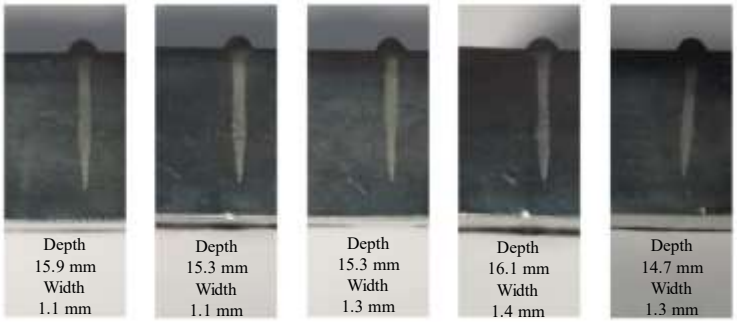


b）Weld quality analysis

Fig.15 Welding line with different anode and cathode distance

Fig.15 shows that within the selected range, as the increase of the cathode-anode distance from 28.5 mm to 29.3 mm, the aspect ratio of the weld decreases from 14.45 to 11.3. Combined with the simulation results:the beam spot diameter increases from 0.233 to 0.248mm. The conclusion can be drawn: which proves that under the same beam current, with the increase in cathode and anode distance, the beam spot diameter gradually increases, eventually leading to an decrease in the weld depth to width ratio.

### *4.3 Anode aperture*

To study the influence of anode aperture on the the aspect ratio of the weld, the anode aperture is 8.5, 9.0, 9.5, 10.0, and 10.5 mm for testing. Moreover, the distance between the cathode and anode is 29.3mm. And the diameter of the bias cup is 5mm. The variation law of the weld aspect ratio with the anode aperture is obtained (shown as Fig.16).

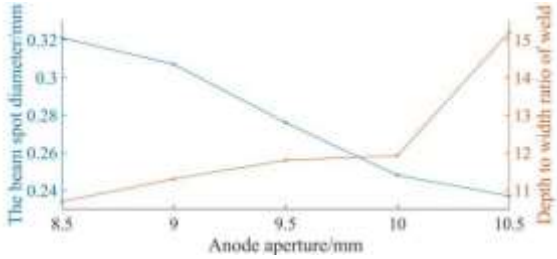


a）Influence of anode aperture on depth to width ratio of weld

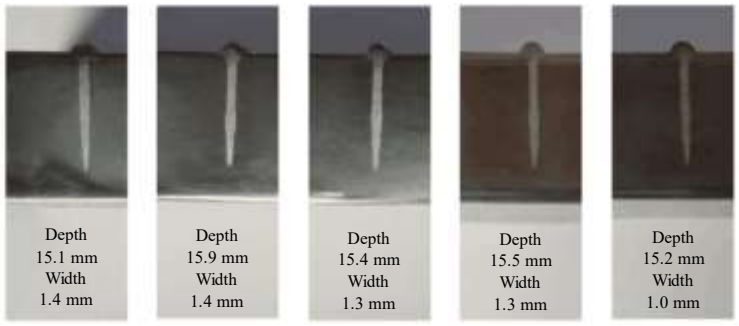


b）Weld quality

Fig.16 Welding line with different anode apertures

Fig.16 illustrates that within the selected range, as the anode aperture increases from 8.5 mm to 10.5 mm, the aspect ratio of the weld increases from 10.78 to 15.2. Combined with the simulation results: the beam spot diameter increases from 0.321 to 0.237mm.The conclusion can be drawn: which proves that under the same beam current, with the increase in bias cup aperture, the diameter of the beam spot becomes smaller， eventually leading to an increase in the weld depth to width ratio.

### *4.4 Focusing current*

The cathode and anode distance is 29.3 mm, the bias cup aperture is 5 mm, and the anode aperture is 10.0 mm. The same test plate is placed at a distance of 100 mm (focusing current 1922 mA), 200 mm (focusing current 1993 mA), 300 mm (focusing current 2066 mA), 400 mm (focusing current 2173 mA) and 500 mm (focusing current 2348 mA) from the working platform for down-beam experiments. The variation law of weld width with focusing current is obtained (shown as Fig.17).

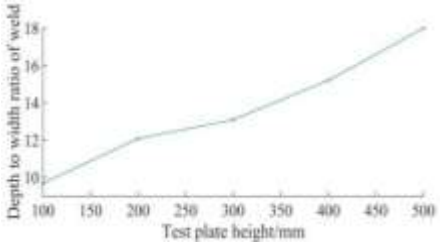


a）Effect of focusing current on weld width

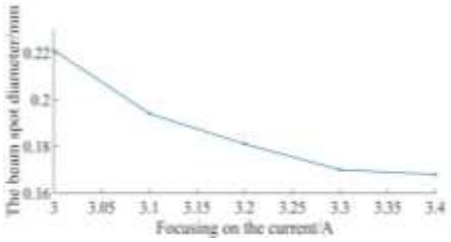


b) Effect of focusing current on the beam spot diameter

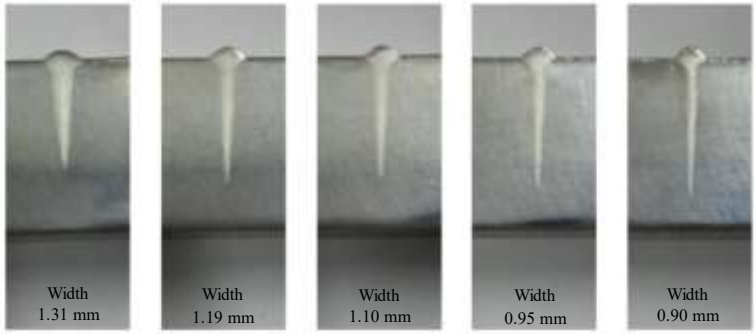


c）Weld width

Fig.17 Weld widths under different focusing current

As can be seen from Fig.17, with the test plate height rising from 100mm (focus current 1.92A) to 500mm (focus current 2.34A)，the aspect ratio of the weld increases from 9.69 to 18，weld width reduced from 1.31mm to 0.9mm. Combined with the simulation results: with the increase of focusing current from 3A to 3.4A, the electron beam spot diameter decreases from 0.22mm to 0.17mm. The conclusion can be drawn: as the focusing current increases, the electron beam spot diameter tends to decrease, which eventually leads to an increase in the electron beam weld depth to width ratio.

The variation trend of electron beam spot diameter under different focusing structures was obtained by numerical analysis, the variation of the electron beam weld depth to width ratio with different focusing structures is then analyzed using experiments. The two trends coincide,which verifies the correctness of the theoretical results and the simulation model.

### *4.5 Orthogonal experiment*

The change in the focusing coil current will cause the height of the beam spot to change. Thus, the aspect ratio of the weld varies sharply. It makes the test results not clear. Therefore, only three parameters including the bias cup aperture, anode aperture, and cathode and anode are considered in this orthogonal experiment. The influences of three parameters on the beam spot are studied. Taking the above three parameters as experimental factors, a three-factor orthogonal experiment is carried out. And four levels are set for each factor. The four-level and three-factor orthogonal test results are shown in Tab.1.

**Tab.1 Four-level three-factor orthogonal test**

| Parameters | | | | Index |
|---|---|---|---|---|
| Number | cathode-anode distance A/mm | Bias cup aperture B/mm | Anode aperture C/mm | Depth to width ratio of weld |
| 01 | 28.4 | 6.0 | 10.0 | 40.4 |
| 02 | 28.4 | 5.5 | 9.5 | 27.14 |
| 03 | 28.4 | 5.0 | 9.0 | 13.67 |
| 04 | 28.4 | 4.5 | 8.5 | 9.93 |
| 05 | 28.7 | 6.0 | 8.5 | 25.125 |
| 06 | 28.7 | 5.5 | 10.0 | 22.25 |
| 07 | 28.7 | 5.0 | 9.5 | 14.57 |
| 08 | 28.7 | 4.5 | 9.0 | 9.73 |
| 09 | 29.0 | 6.0 | 9.0 | 28.157 |
| 10 | 29.0 | 5.5 | 8.5 | 26.285 |
| 11 | 29.0 | 5.0 | 10.0 | 11.48 |
| 12 | 29.0 | 4.5 | 9.5 | 9.93 |
| 13 | 29.3 | 6.0 | 9.5 | 31.833 |
| 14 | 29.3 | 5.5 | 9.0 | 23 |
| 15 | 29.3 | 5.0 | 8.5 | 11.21 |
| 16 | 29.3 | 4.5 | 10.0 | 9.7 |

**Tab.2 Analysis of test results**

| Parameter | | | |
|---|---|---|---|
| | cathode-anode distance A/mm | Bias cup aperture B/mm | Anode aperture C/mm |
| $K_1$ | 91.4 | 125.515 | 83.83 |
| $K_2$ | 71.675 | 98.675 | 83.47 |
| $K_3$ | 75.852 | 50.93 | 73.557 |
| $K_4$ | 75.743 | 39.29 | 72.55 |
| $k_1$ | 22.85 | 31.378 | 20.96 |
| $k_2$ | 17.918 | 24.668 | 20.86 |
| $k_3$ | 18.963 | 12.732 | 18.39 |
| $k_4$ | 18.93 | 9.8 | 18.13 |
| range | 4.932 | 21.573 | 2.83 |
| The optimal solution | 28.4 | 6.0 | 10.0 |

Note: K-the sum of the factor test results , k-the mean of the sum of the factor test results

According to the analysis of the test results in Tab.2, among the three beam source structure parameters, the bias cup aperture has the greatest influence on the beam spot size, followed

by the cathode-anode distance. And the anode aperture has the smallest influence. Moreover, the optimal results within the selection range of the beam source structure is obtained: the distance between the cathode and anode is 28.4 mm, the diameter of the bias cup is 6 mm, and the diameter of the anode is 10 mm.

When the optimal solution is obtained by CST simulation software, the electron gun beam path and electric field distribution are shown in Fig.18. The comparison results of welds before (cathode–anode distance 29.3mm, bias cup aperture 5mm, and anode aperture 10mm)and after optimization are shown in Fig.19.

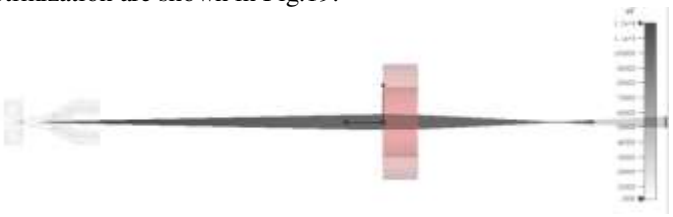

a）Beam path

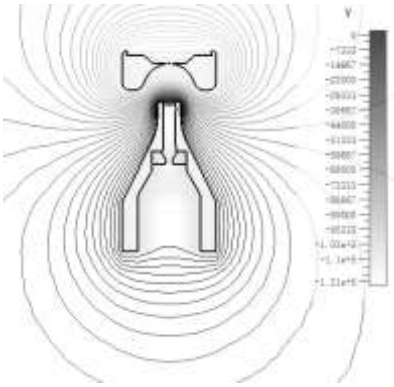

b）Electric field distribution

Fig.18 Beam trajectory and electric field distribution

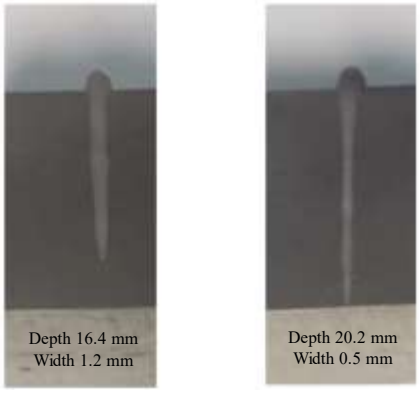


a）Before optimization b) After optimization

Fig.19 Comparison of welds before and after optimization

## 5. Conclusions

1）To solve the problem that there is no systematic theoretical method to calculate the beam waist and beam spot diameters reflecting the focusing characteristics of electron guns, the variation law of electron beam waist and beam spot under different electrostatic focusing structures and magnetic focusing structures is explored by establishing an electron gun on-axis potential model.

2）Using CST simulation software, the changes of electron gun beam waist and beam spot under different electrostatic and magnetic focusing structure parameters are analyzed. What's more, the theoretical analysis results are compared with the simulation results, the two trends coincide.

3）The results of the theoretical and simulation analysis are verified by single-parameter tests. The influences of different parameters on the electron beam spot are explored by designing orthogonal experiments. Theoretical, simulation and experimental comparisons show that the beam spot diameter can be reduced by increasing the aperture of bias cup and anode under the same beam current condition. The spot diameter decreases by increasing the cathode-anode distance. The spot diameter of the beam also decreases with increasing the current of the focusing coil. The bias cup aperture has the greatest influence on the spot diameter. The distance between cathode and anode has the least effect on spot diameter.

4）When the Cathode-anode distance is 28.4 mm, the aperture of bias cup is 6 mm and the aperture of anode is 10 mm, The depth to width ratio of electron beam weld is 40.4；The ratio of weld depth to width before electron gun structure optimization is 13.6，The ratio of weld depth to width was increased by 197%.

**Acknowledgments**-This work was partially supported by the Foreign Cooperation Projects of Fujian Science and Technology Program (Grant No. 2019l0022) and Natural Science Foundation of Fujian Province, China (Grant No.2019J01862). Authors would like to express gratitude to their financial supports.

## References

1. Zhang Yichen. Electron gun and ion beam technology[M]. Beijing: Metallurgical Industry Press, 2004.
2. Zhao Yuqing. Electron beam ion beam technology[M]. Xian:Xi' an Jiaotong University press co., Ltd., 2002.
3. Wang Yan, Zhao Weixia, Deng Chenhui, et al. Design Optimization of Low Energy Electron Gun: A Simulation Study with Hybrid Mesh Model[J]. Chinese Journal of Vacuum Science and Technology, 2020, **40**(1): 1-6.
4. Han Liang, Ning Tao, Li Xiang, et al. The Focusing and Deflecting Characters of e-Type Electron in Heterogeneous Magnetic Field [J]. Xi' an Jiaotong University Xuebao, 2009, (12): 111-114, 119.
5. Wang Xiaoju, Cha Linhong, Qi Kangcheng, et al. Simulation experiment of micro-focus field emission electron gun based on OPERA[J]. Experimental Technology and Management, 2019, **36**(12): 98-101, 106.
6. Huang Weiling, Li Quanfeng, Zhang Kaibin. Characteristics of electron gun used in the accelerator for customs inspection systems[J]. High Power Laser & Particle Beams, 2001,(3): 381-384.
7. Chen Xin, Xu Weiqing, Xu Longquan, et al. Development of an electron gun operated at intermediate-high energies for electron energy-loss spectrometer[J]. Nuclear Techniques, 2017, **40**(5): 10-15.
8. Deng Chenhui, Wang Yan, Liu Junbiao, et al. Property Characterization of Electron Flood Gun with Self-Developed Test Platform[J]. Chinese Journal of Vacuum Science and Technology, 2020, **40**(9): 847-852.
9. Chenhui Deng, Li Han, Yan Wang. Design and Performance of a Miniaturized, Low-Energy, Large Beam Spot Electron Flood Gun[J]. El.ectronics, 2021, **10**(648): 648.
10. Pudjorahardjo, Djoko Slamet, Suprapto, et al. Simulation Study of Electron Beam Spot Size From Thermionic Electron Gun Using SIMION 8.1 Software.[J]. AIP Conference Proceedings, 2018, **2014**(1): 1-9.
11. Qiang Pengfei, Li Linsen, Liu Duo, et al. Gird-control electron gun with multiple focusing electrode[J]. Acta Photonica Sinica, 2016, **45**(4): 0423005.
12. Kornilov S Yu., Osipov I V., Rempe N G. Generation of Narrow Focused Beams in a Plasma-Cathode Electron Gun. Instruments and Experimental Techniques. 2009, **52**(3):406-411.

13. Klimov A S., Burdovitsin V A, Grishkov A A., et al. G.Ribbon Electron Beam Formation by a Forevacuum Plasma Electron Source. Applied Physics. 2015, (1): 35-39.
14. Grishkov A A, Kornilov S Yu, Rempe N G, et al. Shklyaev. Simulation of the formation and transportation of an electron beam in a gas-filled electron-optical system with a plasma emitter. Applied Physics. 2015, (5): 48-53.
15. Xu Haiying, Sang Xinghua, Yang Bo, et al. Development of Novel Cold-Cathode Gas-Discharge Electron Beam Gun:An Instrumentation Study[J]. Chinese Journal of Vacuum Science and Technology, 2021, **41**(3): 284-290.
16. Feng Guangyao, Pei Yuanji, Jiang Daoman, et al. Design of an electron gun in linac for food irradicidation[J]. Nuclear Techniques, 2006, **29**(9): 650-650.
17. Yin Yong, Liu Haijing, Chen Ling, et al. Design of High-Current-Density, Pencil-Beam Electron Gun with Uniform Magnetic Field Focusing[J]. Chinese Journal of Vacuum Science and Technology, 2014, (2): 148-152.
18. Wang Chao, Tang Tiantong, Kang Xiaohui, Modulating properties of electrostatic immersion objective laminar flow gun[J]. High Power Laser & Particle Beams, 2008, (4): 661-665.

## Statements & Declarations

• All data generated or analysed during this study are included in this published article [and its supplementary information files].

# Supplementary Files

This is a list of supplementary files associated with this preprint. Click to download.

- Rawdata.docx